RSC Advances

PAPER

View Article Online
View Journal | View Issue

Cite this: *RSC Adv.*, 2015, **5**, 21012

Synthesis, optical, electrochemical and photovoltaic properties of a D–π–A fluorescent dye with triazine ring as electron-withdrawing anchoring group for dye-sensitized solar cells

Yousuke Ooyama,* Koji Uenaka and Joji Ohshita*

The D–π–A fluorescent dye **OUJ-1** with 1,3,5-triazine ring as electron-withdrawing anchoring group and (diphenylamino)carbazole containing a thiophene ring as D–π moiety have been newly developed and their optical and electrochemical properties, adsorption states on TiO_2 nanoparticles, and photovoltaic performance in dye-sensitized solar cell (DSSC) were investigated. The absorption maximum (λ_{max}^{abs}) for the intramolecular charge-transfer (ICT) absorption band of the D–π–A dye **OUJ-1** occurs at a longer wavelength than those of D–π–A dye **NI-6** with a pyridyl group and D–π–A dye **OUK-1** with a pyrzayl group. Moreover, the dye **OUJ-1** exhibits significant fluorescence solvatochromic properties, that is, a bathochromic shift of the fluorescence band and a decrease in the fluorescence quantum yield (Φ) due to a change from the ^{1}ICT excited state to the twisted intramolecular charge transfer (TICT) excited state with increasing solvent polarity were observed. The photovoltaic performance of a DSSC based on **OUJ-1** is lower than those of **NI-6** and **OUK-1** due to the low dye loading of **OUJ-1** on TiO_2 electrode. It was found that the dye **OUJ-1** is adsorbed onto the TiO_2 surface through the formation of trizainium ions at the Brønsted acid sites (surface-bound hydroxyl groups, Ti–OH) on the TiO_2 surface, although the dye **NI-6** was predominantly adsorbed on the TiO_2 through coordinate bonding between the pyridyl group of the dye and the Lewis acid sites (exposed Ti^{n+} cations) on the TiO_2 surface, and the dye **OUK-1** was adsorbed on the TiO_2 surface through both the formations of hydrogen bonding of pyrazyl groups and pyrazinium ions at Brønsted acid sites on the TiO_2 surface. This work revealed that the binding mode of D–π–A dye sensitizers with azine rings on the TiO_2 surface can be changed by control of the basicity and electron density of the azine rings.

Received 15th December 2014
Accepted 16th February 2015

DOI: 10.1039/c4ra16399k

www.rsc.org/advances

Introduction

Donor–acceptor π-conjugated (D–π–A) fluorescent dyes having both electron-donating (D) and -accepting (A) groups linked by π-conjugated bridges are useful as emitters for organic light emitting diodes (OLEDs),[1–3] photosensitizers for dye-sensitized solar cells (DSSCs),[4–6] and fluorescence sensors for a variety of applications,[7–9] because of their strong absorption and emission properties originating from the intramolecular charge transfer (ICT) excitation from the donor to acceptor moiety in the D–π–A structures. As a noteworthy structural feature of D–π–A dyes, the highest occupied molecular orbital (HOMO) is localized over the π-conjugated system close to the donor part, and the lowest unoccupied molecular orbital (LUMO) is localized over the acceptor part. In the light of the D–π–A structure concept, the expansion of π conjugation and the increase in the electron-donating and electron-accepting abilities of donors (D) and acceptors (A), respectively, leads to the decrease in the energy gap between the HOMO and LUMO. Thus, the photophysical, electrochemical, and ICT properties of a D–π–A dye strongly depend on the electron-donating ability of D and the electron-accepting ability of A, as well as on the electronic characteristics of the π bridge, that is, they should be strategically tunable through chemical modification on each component (D, A, or π bridge) to suit the requirements for efficient optoelectronic devices and optical, biochemical, and medicinal sensors.

In this work, D–π–A fluorescent dye **OUJ-1** with 1,3,5-triazine ring as electron-withdrawing anchoring group and (diphenylamino)carbazole containing a thiophene ring as D–π moiety have been newly developed and their optical and electrochemical properties, adsorption states on TiO_2 nanoparticles, and photovoltaic performances in DSSC were investigated (Scheme 1). The absorption maximum (λ_{max}^{abs}) for the ICT absorption band of the D–π–A dye **OUJ-1** occurs at a longer wavelength than those of D–π–A dye **NI-6** with a pyridyl group[10] and D–π–A dye **OUK-1** with a pyrzayl group.[11] Moreover, the dye

Department of Applied Chemistry, Graduate School of Engineering, Hiroshima University, Higashi-Hiroshima 739-8527, Japan. E-mail: yooyama@hiroshima-u.ac.jp; Fax: (+81) 82-424-5494

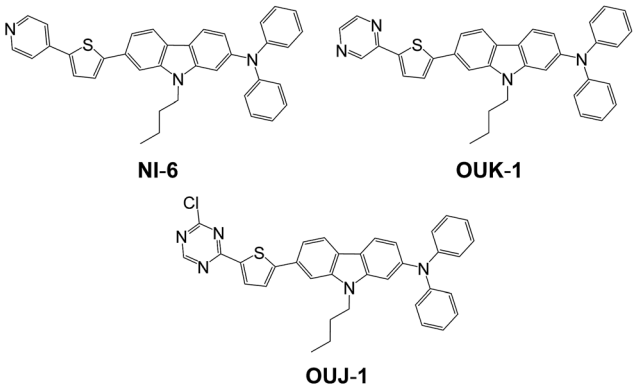

Scheme 1 Chemical structures of D–π–A dye sensitizers **NI-6**, **OUK-1** and **OUJ-1** with azine rings.

OUJ-1 exhibits significant fluorescence solvatochromic properties. It was found that the dye **OUJ-1** is adsorbed onto the TiO_2 surface through the formation of trizainium ion at the Brønsted acid sites (surface-bound hydroxyl groups, Ti–OH) on TiO_2 surface, although the dye **NI-6** was predominantly adsorbed on the TiO_2 through coordinate bonding between the pyridyl group of the dye and the Lewis acid site (exposed Ti^{n+} cations) on the TiO_2 surface, and the dye **OUK-1** was adsorbed on the TiO_2 surface through both the formations of hydrogen bonding of pyrazyl group and pyrazinium ion at Brønsted acid sites on the TiO_2 surface. The photovoltaic performance of DSSC based on **OUJ-1** is lower those of **NI-6** and **OUK-1** due to low dye loading of **OUJ-1** on TiO_2 electrode. On the basis of the experimental results and molecular orbital calculations, the differences of optical and electrochemical properties, adsorption states on TiO_2 nanoparticles, and photovoltaic performances in DSSC among these D–π–A dyes with azine rings are discussed.

Results and discussion

Synthesis

The synthesis of **NI-6** and **OUK-1** have been reported elsewhere.[10a,11] The synthetic pathway of D–π–A fluorescent dye **OUJ-1** is shown in Scheme 2. The dye **OUJ-1** was prepared by Stille coupling of stannyl compound **1** (ref. 11) with 2,4-dichloro-1,3,5-triazine.

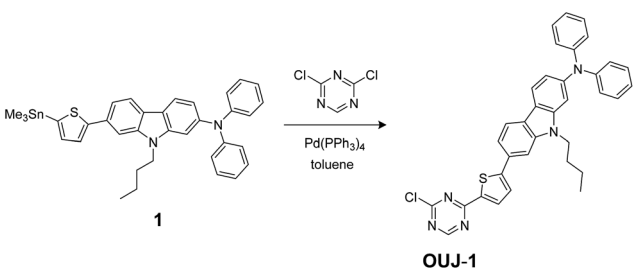

Scheme 2 Synthetic pathway of D–π–A fluorescent dye **OUJ-1** with 1,3,5-triazine ring.

Optical properties

The absorption and fluorescence spectra of **NI-6**, **OUK-1**, **OUJ-1** in various solvents are shown in Fig. 1 and their spectral data are summarized in Table 1. The three dyes in 1,4-dioxane show the absorption maximum (λ_{max}^{abs}) at around 395–430 nm, which is assigned to the ICT excitation from electron donor moiety (diphenylamino group) to electron acceptor moiety (pyridyl, pyrazyl or trizayl group) (Fig. 1a). The λ_{max}^{abs} for ICT band of the D–π–A dye **OUJ-1** with 2-chloro-1,3,5-triazyl group occurs at a longer wavelength by 35 nm and 29 nm, respectively, than those of D–π–A dye **NI-6** with a pyridyl group and D–π–A dye **OUK-1** with a pyrzayl group, because of stronger electron-withdrawing ability of 2-chloro-1,3,5-triazyl group relative to pyridyl and pyrazyl groups. The molar extinction coefficient (ε) for the ICT band is 49 600 M^{-1} cm^{-1} for **NI-6**, 45 400 M^{-1} cm^{-1} for **OUK-1** and 36 500 M^{-1} cm^{-1} for **OUJ-1**, respectively. The corresponding fluorescence maxima (λ_{max}^{fl}) of **OUJ-1** also occurs at a longer wavelength than those of **NI-6** and **OUK-1**. Interestingly, the dye **OUJ-1** exhibits significant fluorescence solvatochromic properties compared with **NI-6** and **OUK-1**, that is, bathochromic shift of fluorescence band and a decrease in the fluorescence quantum yields (Φ) with increasing solvent polarity were

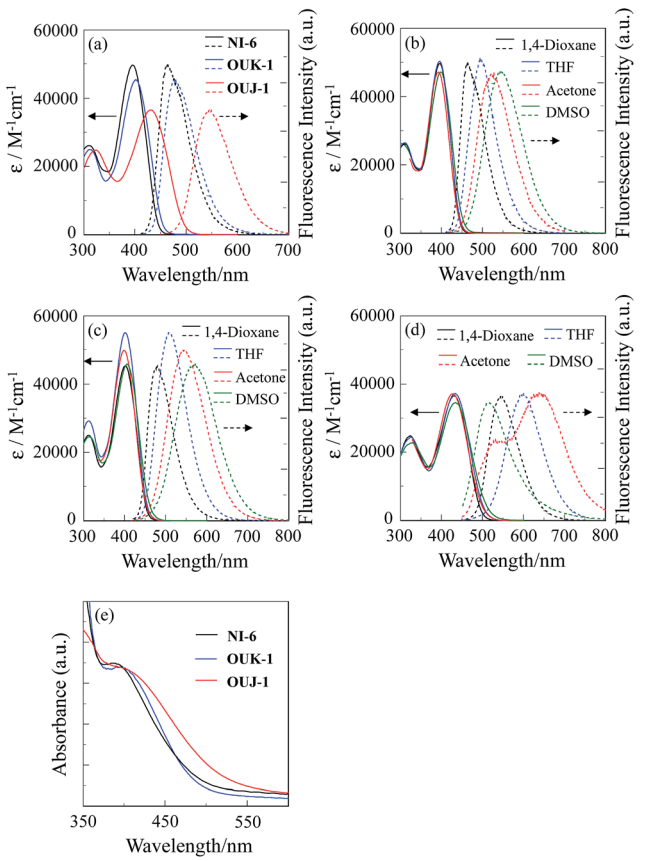

Fig. 1 (a) Absorption (—) and fluorescence (···) spectra of **NI-6**, **OUK-1** and **OUJ-1** in 1,4-dioxane. Absorption (—) and fluorescence (···) spectra of (b) **NI-6**, (c) **OUK-1** and (d) **OUJ-1** in 1,4-dioxane, THF, acetone and DMSO. (e) Absorption spectra of **NI-6**, **OUK-1** and **OUJ-1** adsorbed on TiO_2 film.

Table 1 Optical data of **NI-6**, **OUK-1** and **OUJ-1**

Dye	Solvent	λ_{max}^{abs} [a]/nm (ε M^{-1} cm^{-1})	λ_{max}^{fl} [a]/nm (Φ_f)	Stokes shift cm^{-1}
NI-6	1,4-Dioxane	396 (49 600)	464 (0.58)	3700
	THF	395 (49 900)	495 (0.77)	5114
	Acetone	393 (48 000)	528 (0.58)	6505
	DMSO	399 (47 100)	547 (0.68)	6781
OUK-1	1,4-Dioxane	402 (45 400)	478 (0.46)	3955
	THF	402 (55 000)	508 (0.68)	5190
	Acetone	399 (49 800)	542 (0.56)	6612
	DMSO	406 (45 800)	572 (0.55)	7148
OUJ-1	1,4-Dioxane	431 (36 500)	547 (0.57)	5780
	THF	433 (37 200)	600 (0.63)	6428
	Acetone	428 (37 200)	638 (0.06)	7690
	DMSO	434 (34 500)	516 (<0.02)	3661

[a] Fluorescence quantum yields (Φ_f) were determined by using a calibrated integrating sphere system (the observed λ_{max}^{abs} in each solvent was used as the excitation wavelengths).

observed, although the absorption spectra are nearly independent of solvent polarity (Fig. 1b–d). In low polar solvent such as 1,4-dioxane and THF, the dye **OUJ-1** exhibits fluorescence band at 547 nm in 1,4-dioxane and 600 nm in THF, respectively, arising from the ^{1}ICT excited state. In polar solvent such as acetone, on the other hand, a new fluorescence band with the a significant decrease in the Φ value appeared at 638 nm, arising from the twisted intramolecular charge transfer (TICT) excited state which is due to the twisting between the triazyl group and the (diphenylamino)carbazole moiety, leading to non-radiative deactivation. Moreover, in highly polar solvent such as DMSO, owing to significant non-radiative deactivation from the TICT excited state leading to a decrease in the Φ value, the fluorescence band from only the ^{1}ICT excited state was observed at 516 nm. Consequently, this result suggested that the predominant excited state for the D–π–A fluorescent dye **OUJ-1** with triazyl group, which possesses stronger electron-withdrawing ability than those of pyridyl and pyrazyl groups, changes from the ^{1}ICT state to the TICT state with increasing solvent polarity, resulting in a significant fluorescence solvatochromism.[12,13]

The absorption spectra of **NI-6**, **OUK-1** and **OUJ-1** adsorbed on TiO_2 film are shown in Fig. 1e. The absorption band of **OUJ-1** are broadened compared with those of **NI-6** and **OUK-1**. However, the absorption peak wavelengths of the three dyes adsorbed on TiO_2 are similar to those in 1,4-dioxane, although the absorption bands of the three dyes adsorbed on the TiO_2 film are broadened compared with those in 1,4-dioxane. Thus, this result indicates that the three dyes form weak π-stacked aggregates on TiO_2 surface.

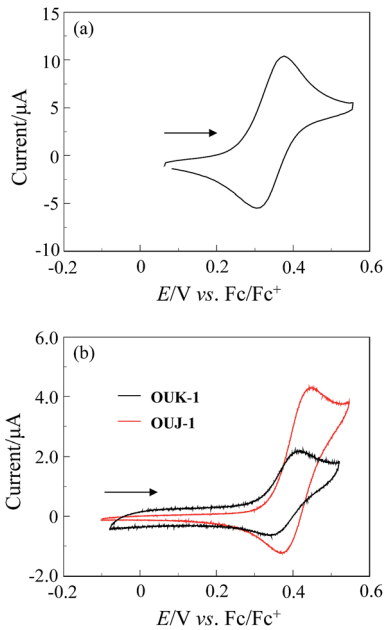

Fig. 2 Cyclic voltammograms of (a) **NI-6** in CH_2Cl_2 containing 0.1 M Bu_4NClO_4 and (b) **OUK-1** and **OUJ-1** in DMF containing 0.1 M Bu_4NClO_4. The arrow denotes the direction of the potential scan.

Electrochemical properties

The electrochemical properties of **NI-6**, **OUK-1** and **OUJ-1** and were determined by cyclic voltammetry (CV). The CV curve of the three dyes are shown in Fig. 2. The reversible oxidation waves for the three dyes were observed at 0.37 V for **NI-6**, 0.42 V for **OUK-1**, 0.45 V for **OUJ-1**, respectively, *vs.* ferrocene/ferrocenium (Fc/Fc^+) (Table 2). The corresponding reduction

Table 2 Electrochemical data and HOMO and LUMO energy levels of **NI-6**, **OUK-1** and **OUJ-1**

Dye	E_{pa}/V[a]	E_{pc}/V[a]	$E_{1/2}^{ox}$/V[a]	HOMO/V[b]	LUMO/V[b]
NI-6	0.37	0.30	0.34	0.97	−1.87
OUK-1	0.42	0.35	0.39	1.11	−1.68
OUJ-1	0.45	0.37	0.41	1.13	−1.40

[a] Anodic (E_{pa}) and cathodic (E_{pc}) peak potentials, and half-wave potentials for oxidation ($E_{1/2}^{ox}$) *vs.* Fc/Fc^+ were recorded in CH_2Cl_2/Bu_4NClO_4 (0.1 M) solution for **NI-6** and DMF/Bu_4NClO_4 (0.1 M) solution for **OUK-1** and **OUJ-1**, respectively. [b] *vs.* normal hydrogen electrode (NHE).

waves appeared at 0.30 V for **NI-6**, 0.35 V for **OUK-1** and 0.37 V for OUJ-1, respectively, thus showing that the oxidized states of the three dyes are stable. The HOMO energy level *vs.* the normal hydrogen electrode (NHE) was evaluated from the half-wave potential for oxidation ($E^{ox}_{1/2}$ = 0.34 V for **NI-6**, 0.39 V for **OUK-1** and 0.41 V for **OUJ-1**). The HOMO energy level was 0.97 V for **NI-6**, 1.11 V for **OUK-1** and 1.13 V for **OUJ-1**, respectively, *vs.* NHE, thus indicating that the three dyes have comparable HOMO energy levels. This result shows that the HOMO energy levels are more positive than the I_3^-/I^- redox potential (0.4 V), and thus this ensures an efficient regeneration of the oxidized dyes by electron transfer from the I_3^-/I^- redox couple in the electrolyte. The LUMO energy level was estimated from the $E^{ox}_{1/2}$ and an intersection of absorption and fluorescence spectra (436 nm; 2.84 eV for **NI-6**, 445 nm; 2.79 eV for **OUK-1**, 491 nm; 2.52 eV for **OUJ-1**) in 1,4-dioxane, that is, the LUMO energy level was obtained through eqn – [E_{0-0} – HOMO], where E_{0-0} transition energy is an intersection of absorption and fluorescence spectra corresponding to the energy gap between HOMO and LUMO, and HOMO *vs.* NHE was evaluated from the $E^{ox}_{1/2}$ value. The LUMO energy levels decrease in the order of **NI-6** (−1.87 V) > **OUK-1** (−1.68 V) > **OUJ-1** (−1.40 V), showing that the lowering of LUMO energy levels is dependent on the electron-withdrawing ability of azine ring. Consequently, it was revealed that the red-shift of the ICT absorption band for **OUJ-1** relative to **NI-6** and **OUK-1** is attributed to stabilization of the LUMO level because of stronger electron-withdrawing ability of triazyl group relative to pyridyl and pyrazyl groups, resulting in a decrease in the HOMO–LUMO band gap. Evidently, the LUMO energy levels of the three dyes are higher than the energy level (E_{cb}) of the CB of TiO_2 (−0.5 V), suggesting that an electron injection to the CB of TiO_2 is thermodynamically feasible.

Theoretical calculations

In order to examine the electronic structures of **NI-6**, **OUK-1** and **OUJ-1**, the molecular orbitals of the three dyes were calculated using density functional theory (DFT) at the B3LYP/6-31G(d, p) level. The DFT calculations indicate that for the three dyes the HOMOs were mostly localized on the (diphenylamino)carbazole containing a thiophene ring, and the LUMOs were mostly localized on the thienylpyridine for **NI-6**, thienylpyrazine for **OUK-1** and thienyltriazine for **OUJ-1**, respectively (Fig. 3). Accordingly, the DFT calculations reveal that dye excitations upon light irradiation induce a strong ICT from the (diphenylamino)carbazole to the azine ring.

FTIR spectra

To elucidate the adsorption states of **OUJ-1** on TiO_2 nanoparticles, we measured the FTIR spectra of the dye powders and the dyes adsorbed on TiO_2 nanoparticles (Fig. 4). In our previous study, it was found that the dye **NI-6** was predominantly adsorbed on the TiO_2 through coordinate bonding between the pyridyl group of the dye and the Lewis acid site (exposed Ti^{n+} cations) on the TiO_2 surface, and the dye **OUK-1** was adsorbed on the TiO_2 through both the formations of hydrogen bonding of pyrazyl group and pyrazinium ion at Brønsted acid sites (surface-bound hydroxyl groups, Ti–OH) on the TiO_2 surface, where the adsorption amount of the dye adsorbed on TiO_2 electrode is 3.1×10^{16} and 3.0×10^{16} molecules per cm^2 for **NI-6** and **OUK-1**, respectively.[10a,11] For the powders of **OUJ-1**, the C=N stretching band of trizaine ring was clearly observed at 1536 cm^{-1}. When the dye **OUJ-1** was adsorbed on the TiO_2 surface, where the adsorption amount of the dye adsorbed on TiO_2 electrode is 2.5×10^{16} molecules per cm^2, the band at 1536 cm^{-1} disappeared completely and a new band appeared at around 1650 cm^{-1}, indicating that the dye **OUJ-1** is adsorbed onto the TiO_2 through the formation of trizainium ion at the Brønsted acid sites on TiO_2 surface. These results suggest that the binding modes of D–π–A dye sensitizers with azine rings on TiO_2 surface can be changed by control of the basicity and electron density of azine rings.

Dye-sensitized solar cells

The DSSCs were fabricated by using the dye-adsorbed TiO_2 electrode (9 μm), Pt-coated glass as a counter electrode, and an acetonitrile solution with iodine (0.05 M), lithium iodide (0.1 M), and 1,2-dimethyl-3-propylimidazolium iodide (0.6 M) as an electrolyte. The photocurrent–voltage (*I–V*) characteristics were measured under simulated solar light (AM 1.5, 100 mW cm^{-2}). The incident photon-to-current conversion efficiency (IPCE) spectra and the *I–V* curves are shown in Fig. 5. The photovoltaic performance parameters are collected in Table 3. The adsorption amount of dyes adsorbed on TiO_2 is 3.0×10^{16} and 2.5×10^{17} molecules per cm^2 for **OUK-1** and **OUJ-1**, respectively, when

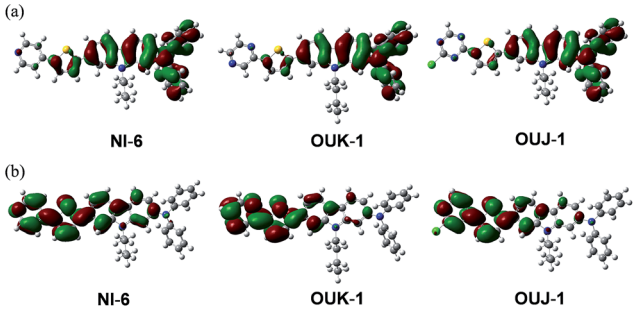

Fig. 3 (a) HOMO and (b) LUMO of **NI-6**, **OUK-1** and **OUJ-1** by the density functional theory (DFT) calculations at B3LYP/6-31G(d, p) level.

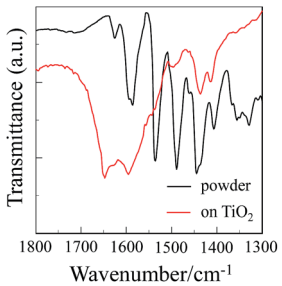

Fig. 4 FTIR spectra of the dye powders and the dyes (2.5×10^{16} molecules per cm^2) adsorbed on TiO_2 nanoparticles for **OUJ-1**.

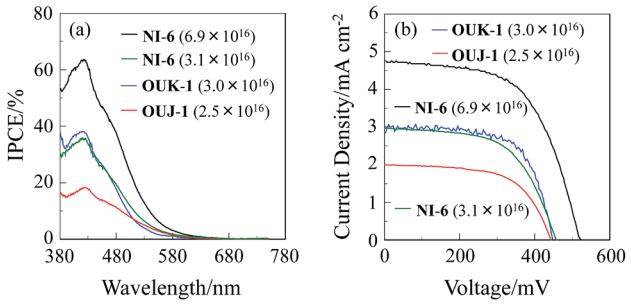

Fig. 5 (a) IPCE spectra and (b) *I*–*V* curves and of DSSCs based on **NI-6**, **OUK-1** and **OUJ-1**. The adsorption amount of the dye adsorbed on TiO_2 electrode is 3.1×10^{16} and 6.9×10^{16} molecules per cm^2 for **NI-6**, and 3.0×10^{16} and 2.5×10^{16} molecules per cm^2 for **OUK-1** and **OUJ-1**, respectively.

Table 3 DSSC performance parameters of **NI-6**, **OUK-1** and **OUJ-1**

Dye	Molecules[a] cm^{-2}	J_{sc}[e]/mA cm^{-2}	V_{oc}[e]/mV	FF[e]	η[e] (%)
NI-6	6.9×10^{16}[b]	4.76	523	0.59	1.47
	3.1×10^{16}[c]	2.96	460	0.58	0.79
OUK-1	3.0×10^{16}[d]	2.99	448	0.67	0.89
OUJ-1	2.5×10^{16}[d]	2.00	444	0.61	0.54

[a] The 9 μm thick TiO_2 electrode was immersed into dye solution in THF. [b] Under the adsorption condition of 0.1 mM dye solution in THF. [c] Under the adsorption condition of 0.06 mM dye solution in THF. [d] Under the adsorption condition of 1.0 mM dye solution in THF. [e] Under a simulated solar light (AM 1.5, 100 mW cm^{-2}).

the TiO_2 electrode was immersed into 1.0 mM dye solution of **OUK-1** or **OUJ-1**. It is worth mentioning here that the adsorption amounts of **NI-6** on the co-adsorbed TiO_2 electrode is 3.1×10^{16} molecules cm^{-2}, which is equivalent to that of **OUK-1** and **OUJ-1** under the adsorption condition of 0.1 mM dye solution, when the TiO_2 electrode was immersed into dye **NI-6** solution as low as 0.06 mM. Moreover, the adsorption amount of **NI-6** reached as high as 6.9×10^{16} molecules cm^{-2} under the adsorption condition of 0.1 mM dye solution. The difference in adsorption ability onto TiO_2 surface among the three dyes may be associated with the basicity and electron density of azine rings,

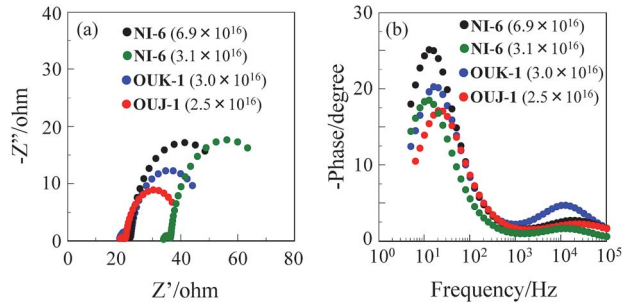

Fig. 6 (a) Nyquist plots and (b) Bode phase plots of DSSCs based on **NI-6**, **OUK-1** and **OUJ-1**. The adsorption amount of the dye adsorbed on TiO_2 electrode is 3.1×10^{16} and 6.9×10^{16} molecules per cm^2 for **NI-6**, and 3.0×10^{16} and 2.5×10^{16} molecules per cm^2 for **OUK-1** and **OUJ-1**, respectively.

leading to changes of the binding modes of azine rings on TiO_2 surface. Consequently, this result indicates that the pyridyl unit is better anchoring group for achieving high dye loading than pyrazyl and triazyl group. When the adsorption amount of the dye is 2.5–3.1 $\times 10^{16}$ molecules per cm^2, the maximum IPCE value at around 420 nm increases in the order of **OUJ-1** (18%) < **NI-6** (36%) ≈ **OUK-1** (38%) (Fig. 5a). The short-circuit photocurrent density (J_{sc}) and solar energy-to-electricity conversion yield (η) also increase in the order of **OUJ-1** (2.00 mA cm^{-2}, 0.54%) < **NI-6** (2.96 mA cm^{-2}, 0.79%) ≈ **OUK-1** (2.99 mA cm^{-2}, 0.89%) (Fig. 5b and Table 2). The lower photovoltaic performances for DSSC based on **OUJ-1** are attributed to low adsorption amount of the dyes on TiO_2 electrode. On the other hand, the DSSC based on **NI-6**-adsorbed TiO_2 electrode with 6.9 $\times 10^{16}$ molecules per cm^2 showed the J_{sc} (4.76 mA cm^{-2}), η values (1.47%) and maximum IPCE value (64% at 420 nm), which are twice as high as those of low adsorption amount of the dye (3.1×10^{16} molecules cm^{-2}) due to the enhancement of LHE with increasing dye loading on TiO_2 electrode. Moreover, the open-circuit photovoltage (V_{oc}) for DSSCs based on **OUK-1** (448 mV) and **OUJ-1** (444 mV) is lower than that of **NI-6** (460 mV and 523 mV for 3.1×10^{16} and 6.9×10^{16} molecules per cm^2, respectively). Thus, electrochemical impedance spectroscopy (EIS) analysis was performed to study the electron recombination process in DSSCs in the dark under a forward bias of −0.45 V or −0.60 V with a frequency range of 10 mHz to 100 kHz. The large semicircle in the Nyquist plot (Fig. 6a), which corresponds to the midfrequency peaks in the Bode phase plots, represents the charge recombination between the injected electrons in TiO_2 and I_3^- ions in the electrolyte, that is, the charge-transfer resistances at the TiO_2/dye/electrolyte interface. The Nyquist plots show that the resistance value of the large semicircle for **NI-6** (44 Ω and 50 Ω for 3.1×10^{16} and 6.9×10^{16} molecules per cm^2, respectively) is larger than those of **OUK-1** (26 Ω) and **OUJ-1** (20 Ω), indicating that the electron recombination resistance of **NI-6** is higher than those of those of **OUK-1** and **OUJ-1**. The electron recombination lifetimes (τ_e) expressing the electron recombination between the injected electrons in TiO_2 and I_3^- ions in the electrolyte, extracted from the angular frequency (ω_{rec}) at the midfrequency peak in the Bode phase plot (Fig. 6b) using $\tau_e = 1/\omega_{rec}$, are 16 ms for both DSSCs based on **NI-6**-adsorbed TiO_2 electrode with 3.1×10^{16} and 6.9×10^{16} molecules per cm^2, which is larger than 10 ms and 8 ms for DSSCs based on **OUK-1** and **OUJ-1**, respectively. Thus, this result revealed that the charge recombination between the injected electrons in TiO_2 and I_3^- ions in the electrolyte is not major reason for the difference in V_{oc} value between the three dyes, but the negative shift of the E_{cb} of TiO_2 by the formations of coordinate bonding between the pyridyl group of the dye and the Lewis acid site on the TiO_2 surface may result in a higher V_{oc} value for **NI-6**.[6]

Conclusions

We have designed and synthesized D–π–A fluorescent dye **OUJ-1** with 1,3,5-triazine ring as electron-withdrawing anchoring group and (diphenylamino)carbazole containing a thiophene

ring as D–π moiety. The dye **OUJ-1** exhibits significant fluorescence solvatochromic properties due to change from the ^{1}ICT excited state to the TICT excited state with increasing solvent polarity, compared with D–π–A dye **NI-6** with a pyridyl group and D–π–A dye **OUK-1** with a pyrzayl group. It was found the dye **OUJ-1** is adsorbed onto the TiO_2 surface through the formation of trizainium ion at the Brønsted acid sites on TiO_2 surface, although the dye **NI-6** was predominantly adsorbed on the TiO_2 through coordinate bonding between the pyridyl group of the dye and the Lewis acid site on the TiO_2 surface, and the dye **OUK-1** was adsorbed on the TiO_2 surface through both the formations of hydrogen bonding of pyrazyl group and pyrazinium ion at Brønsted acid sites on the TiO_2 surface. The photovoltaic performance of DSSC based on **OUJ-1** is lower those of **NI-6** and **OUK-1** due to low dye loading of **OUJ-1** on TiO_2 electrode. In addition, our results indicate that the pyridyl unit is better anchoring group for achieving high dye loading than pyrazyl and triazyl group. Consequently, this work suggests that the binding modes of D–π–A dye sensitizers with azine rings on TiO_2 surface can be changed by control of the basicity and electron density of azine rings. Further studies to ensure this conclusion are now in progress by estimating pK_a values of D–π–A dye sensitizers with azine rings.

Experimental

General

Melting points were measured with a Yanaco micro melting point apparatus MP model. IR spectra were recorded on a Perkin Elmer Spectrum One FT-IR spectrometer by ATR method. High-resolution mass spectral data were acquired on a Thermo Fisher Scientific LTQ Orbitrap XL. ^{1}H NMR spectra were recorded on a Varian-400 (400 MHz) FT NMR spectrometer. Absorption spectra were observed with a Shimadzu UV-3150 spectrophotometer and fluorescence spectra were measured with a HORIBA FluoroMax-4 spectrofluorometer. The fluorescence quantum yields in solution were determined by a HORIBA FluoroMax-4 spectrofluorometer by using a calibrated integrating sphere system. Cyclic voltammetry (CV) curves were recorded in CH_2Cl_2/Bu_4NClO_4 (0.1 M) solution for **NI-6** and DMF/Bu_4NClO_4 (0.1 M) solution for **OUJ-1** and **OUJ-1**, respectively, with a three-electrode system consisting of Ag/Ag^+ as reference electrode, Pt plate as working electrode, and Pt wire as counter electrode by using a AMETEK Versa STAT 4 potentiostat. The highest occupied molecular orbital (HOMO) and lowest unoccupied molecular orbital (LUMO) energy levels of **NI-6**, **OUK-1** and **OUJ-1** were evaluated from the spectral analyses and the CV data (the HOMO energy level was evaluated from the $E^{ox}_{1/2}$). The LUMO energy level was estimated from the $E^{ox}_{1/2}$ and an intersection of absorption and fluorescence spectra (436 nm; 2.84 eV for **NI-6**, 445 nm; 2.79 eV for **OUK-1**, 491 nm; 2.52 eV for **OUJ-1**) in 1,4-dioxane, that is, the LUMO energy level was obtained through eqn – [E_{0-0} − HOMO], where E_{0-0} transition energy is an intersection of absorption and fluorescence spectra corresponding to the energy gap between HOMO and LUMO, and HOMO *vs.* NHE was evaluated from the $E^{ox}_{1/2}$ value. Electrochemical impedance spectroscopy (EIS) for DSSCs in the dark under a forward bias of −0.60 V for **NI-6** and **OUK-1** and −0.45 V for **OUJ-1** with a frequency range of 10 mHz to 100 kHz was measured with a AMETEK Versa STAT 3.

Synthesis

9-Butyl-7-(5-(4-chloro-1,3,5-triazin-2-yl)thiophen-2-yl)-*N*,*N*-diphenyl-9*H*-carbazol-2-amine (OUJ-1). A solution of **1** (ref. 11) (0.34 g, 0.53 mmol), 2,4-dichloro-1,3,5-triazine (0.09 g, 0.58 mmol), and $Pd(PPh_3)_4$ (0.018 g, 0.016 mmol) in toluene (15 mL) was stirred for 3 h at 110 °C under an argon atmosphere. After concentrating under reduced pressure, the resulting residue was dissolved in dichloromethane and washed with water. The dichloromethane extract were evaporated under reduced pressure. The residue was chromatographed on silica gel (ethyl acetate–hexane = 1 : 6 as eluent as eluent) to give **OUJ-1** (0.13 g, yield 42%) as a yellow solid; m.p. 201–202 °C; IR (ATR): $\tilde{\nu}$ = 1586, 1536, 1488, 1444 cm^{-1}; ^{1}H NMR (400 MHz, CD_2Cl_2) δ = 0.88 (t, J = 7.4 Hz, 3H), 1.26–1.33 (m, 2H), 1.73–1.80 (m, 2H), 4.19 (t, J = 7.0 Hz, 2H), 6.95 (dd, J = 1.6 and 8.4 Hz, 1H), 7.02–7.06 (m, 2H), 7.12–7.16 (m, 5H), 7.25–7.30 (m, 4H), 7.56 (d, J = 4.0 Hz, 1H), 7.58 (dd, J = 1.6 and 8.1 Hz, 1H), 7.69 (d, J = 1.2 Hz, 1H), 7.94 (d, J = 8.4 Hz, 1H), 8.03 (d, J = 8.1 Hz, 1H), 8.24 (d, J = 4.0 Hz, 1H), 8.89 (s, 1H); HRMS (APCI): *m*/*z* (%): [M + H$^+$] calcd for $C_{35}H_{29}N_5ClS$, 586.18267; found 586.18292.

Preparation of DSSCs

The TiO_2 paste (JGC Catalysts and Chemicals Ltd., PST-18NR) was deposited on a fluorine-doped-tin-oxide (FTO) substrate by doctor-blading, and sintered for 50 min at 450 °C. The 9 μm thick TiO_2 electrode was immersed into 0.06 mM or 0.1 mM dye (**NI-6**) solution in THF or 1.0 mM dye (**OUK-1** and **OUJ-1**) solution in THF for 15 hours enough to adsorb the dye sensitizers. The DSSCs were fabricated by using the TiO_2 electrode (0.5 × 0.5 cm^2 in photoactive area) thus prepared, Pt-coated glass as a counter electrode, and a solution of 0.05 M iodine, 0.1 M lithium iodide, and 0.6 M 1,2-dimethyl-3-propylimidazolium iodide in acetonitrile as electrolyte. The photocurrent–voltage characteristics were measured using a potentiostat under a simulated solar light (AM 1.5, 100 mW cm^{-2}). IPCE spectra were measured under monochromatic irradiation with a tungsten–halogen lamp and a monochromator. The dye-coated film for **NI-6** and **OUK-1** was immersed in a mixed solvent of THF–DMSO–NaOH aq. 1 M (5 : 4 : 1), which was used to determine the amount of dye molecules adsorbed onto the film by measuring the absorbance. The quantification of dye was made based on the molar extinction coefficient for λ^{abs}_{max} of dye in the above solution. For **OUJ-1**, the amount of adsorbed dye on TiO_2 nanoparticles was determined form the calibration curve by absorption spectral measurement of the concentration change of the dye solution before and after adsorption, because the dye **OUJ-1** is decomposed by the mixed solvent of THF–DMSO–NaOH aq. 1 M (5 : 4 : 1). Absorption spectra of the dyes adsorbed on TiO_2 nanoparticles were recorded on the dyes-adsorbed TiO_2 film in the transmission mode with a calibrated integrating sphere system.

Acknowledgements

This work was supported by The Iwatani Naoji Foundation's Research Grant.

Notes and references

1 (*a*) H.-C. Yeh, L.-H. Chan, W.-C. Wu and C.-T. Chen, *J. Mater. Chem.*, 2004, **14**, 1293; (*b*) C.-T. Chen, *Chem. Mater.*, 2004, **16**, 4389; (*c*) G. Hughes and M. R. Bryce, *J. Mater. Chem.*, 2005, **15**, 94; (*d*) S.-L. Lin, L.-H. Chan, R.-H. Lee, M.-Y. Yen, W.-J. Kuo, C.-T. Chen and R.-J. Jeng, *Adv. Mater.*, 2008, **20**, 3947; (*e*) G. Qian, Z. Zhong, M. Luo, D. Yu, Z. Zhang, Z. Y. Wang and D. Ma, *Adv. Mater.*, 2009, **21**, 111.

2 W. Li, L. Yao, H. Liu, Z. Wang, S. Zhang, R. Xiao, H. Zhang, P. Lu, B. Yang and Y. Ma, *J. Mater. Chem. C*, 2014, **2**, 4733.

3 F. Bureš, *RSC Adv.*, 2014, **4**, 58826.

4 (*a*) H. Choi, C. Baik, S. O. Kang, J. Ko, M.-S. Kang, M. K. Nazeeruddin and M. Grätzel, *Angew. Chem., Int. Ed.*, 2008, **47**, 327; (*b*) S. Kim, D. Kim, H. Choi, M.-S. Kang, K. Song, S. O. Kang and J. Ko, *Chem. Commun.*, 2008, 4951; (*c*) W.-H. Liu, I.-C. Wu, C.-H. Lai, C.-H. Lai, P.-T. Chou, Y.-T. Li, C.-L. Chen, Y.-Y. Hsu and Y. Chi, *Chem. Commun.*, 2008, 5152.

5 (*a*) B. Liu, W. Zhu, Q. Zhang, W. Wu, M. Xu, Z. Ning, Y. Xie and H. Tian, *Chem. Commun.*, 2009, 1766; (*b*) G. Li, Y.-F. Zhou, X.-B. Cao, P. Bao, K.-J. Jiang, Y. Lin and L.-M. Yang, *Chem. Commun.*, 2009, 2201; (*c*) H. Choi, I. Raabe, D. Kim, F. Teocoli, C. Kim, K. Song, J.-H. Yum, J. Ko, Md. K. Nazeeruddin and M. Grätzel, *Chem.–Eur. J.*, 2010, **16**, 1193.

6 (*a*) A. Mishra, M. K. R. Fischer and P. Bäuerle, *Angew. Chem., Int. Ed.*, 2009, **48**, 2474; (*b*) Y. Ooyama and Y. Harima, *Eur. J. Org. Chem.*, 2009, **18**, 2903; (*c*) Z. Ning and H. Tian, *Chem. Commun.*, 2009, 5483; (*d*) Z. Ning, Y. Fu and H. Tian, *Energy Environ. Sci.*, 2010, **3**, 1170; (*e*) Y. Ooyama and Y. Harima, *ChemPhysChem*, 2012, **13**, 4032.

7 (*a*) L. Xue, C. Liu and H. Jiang, *Chem. Commun.*, 2009, 1061; (*b*) W. Jiang and W. Wang, *Chem. Commun.*, 2009, 3913; (*c*) M. H. Kim, H. H. Jang, S. Yi, S.-K. Chang and M. S. Han, *Chem. Commun.*, 2009, 4838; (*d*) F. Qian, C. Zhang, Y. Zhang, W. He, X. Gao, P. Hu and Z. Guo, *J. Am. Chem. Soc.*, 2009, **131**, 1460; (*e*) R. Guliyev, A. Coskun and E. U. Akkaya, *J. Am. Chem. Soc.*, 2009, **131**, 9007.

8 Y. Hu, Z. Zhao, X. Bai, X. Yuan, X. Zhangaand and T. Masuda, *RSC Adv.*, 2014, **4**, 55179.

9 Y. I. Park, O. Postupna, A. Zhugayevych, H. Shin, Y.-S. Park, B. Kim, H.-J. Yen, P. Cheruku, J. S. Martinez, J. W. Park, S. Tretiak and H.-L. Wang, *Chem. Sci.*, 2015, **6**, 789.

10 (*a*) Y. Ooyama, S. Inoue, T. Nagano, K. Kushimoto, J. Ohshita, I. Imae, K. Komaguchi and Y. Harima, *Angew. Chem., Int. Ed.*, 2011, **50**, 7429; (*b*) Y. Ooyama, T. Nagano, S. Inoue, I. Imae, K. Komaguchi, J. Ohshita and Y. Harima, *Chem.–Eur. J.*, 2011, **17**, 14837; (*c*) Y. Harima, T. Fujita, Y. Kano, I. Imae, K. Komaguchi, Y. Ooyama and J. Ohshita, *J. Phys. Chem. C*, 2013, **117**, 16364; (*d*) N. Shibayama, H. Ozawa, M. Abe, Y. Ooyama and H. Arakawa, *Chem. Commun.*, 2014, **50**, 6398.

11 Y. Ooyama, K. Uenaka, Y. Harima and J. Ohshita, *RSC Adv*, 2014, **4**, 30225.

12 (*a*) B. Valeur, *Molecular Fluorescence*, VCH, Weinheim, 2002; (*b*) C. Reichardt, *Solvents and Solvent Effects in Organic Chemistry*, VCH, Weinheim, 2003; (*c*) H. Zollinger, *Color Chemistry*, VCH, Weinheim, 2003.

13 (*a*) S. Sumalekshmy and K. R. Gopidas, *J. Phys. Chem. B*, 2004, **108**, 3705; (*b*) S. Sumalekshmy and K. R. Gopidas, *New J. Chem.*, 2005, **29**, 325; (*c*) S. Sumalekshmy and K. R. Gopidas, *Photochem. Photobiol. Sci.*, 2005, **4**, 539; (*d*) Y. Ooyama, G. Ito, K. Kushimoto, K. Komaguchi, I. Imae and Y. Harima, *Org. Biomol. Chem.*, 2010, **8**, 2756.

